J|A|C|S
ARTICLES
Published on Web 07/17/2004

Strong Interfullerene Electronic Communication in a Bisfullerene−Hexarhodium Sandwich Complex

Kwangyeol Lee,*,† Yoon Jeong Choi,‡ Youn-Jaung Cho,‡ Chang Yeon Lee,‡ Hyunjoon Song,‡ Chang Hoon Lee,† Yoon Sup Lee,*,‡ and Joon T. Park*,‡

Contribution from the Department of Chemistry, Korea University, Seoul, 136-701, Korea and National Research Laboratory, Department of Chemistry and School of Molecular Science (BK 21), Korea Advanced Institute of Science and Technology, Daejeon, 305-701, Korea

Received May 10, 2004; E-mail: kylee1@korea.ac.kr, YoonSupLee@kaist.ac.kr, joontpark@kaist.ac.kr

Abstract: Reaction of $Rh_6(CO)_{12}(dppm)_2$ (dppm = 1,2-bis(diphenylphosphino)methane) with 1.4 equiv. of C_{60} in chlorobenzene at 120 °C affords a face-capping C_{60} derivative $Rh_6(CO)_9(dppm)_2(\mu_3\text{-}\eta^2,\eta^2,\eta^2\text{-}C_{60})$ (**1**) in 73% yield. Treatment of **1** with excess CNR (10 equiv., R = $CH_2C_6H_5$) at 80 °C provides a bisbenzylisocyanide-substituted compound $Rh_6(CO)_7(dppm)_2(CNR)_2(\mu_3\text{-}\eta^2,\eta^2,\eta^2\text{-}C_{60})$ (**2**) in 59% yield. Reaction of **1** with excess C_{60} (4 equiv.) in refluxing chlorobenzene followed by treatment with 1 equiv. of CNR at room temperature gives a bisfullerene sandwich complex $Rh_6(CO)_5(dppm)_2(CNR)(\mu_3\text{-}\eta^2,\eta^2,\eta^2\text{-}C_{60})_2$ (**3**) in 31% yield. Compounds **1**, **2**, and **3** have been characterized by spectroscopic and microanalytical methods as well as by X-ray crystallographic studies. Electrochemical properties of **1**, **2**, and **3** have been examined by cyclic voltammetry. The cyclic voltammograms (CVs) of **1** and **2** show two reversible one-electron redox waves, a reversible one-step two-electron redox wave, and a reversible one-electron redox wave, respectively, within the solvent cutoff window. This observation suggests that compounds **1** and **2** undergo similar C_{60}-localized electrochemical pathways up to $\mathbf{1}^{5-}$ and $\mathbf{2}^{5-}$. Each redox wave of **2** appears at more negative potentials compared to that of **1** because of the donor effect of the benzylisocyanide ligand. The CV of compound **3** reveals six reversible well-separated redox waves due to strong interfullerene electronic communication via the Rh_6 metal cluster bridge. The electrochemical properties of **1**, **2**, and **3** have been rationalized by molecular orbital calculations using the density functional theory (DFT) method. In particular, the molecular orbital (MO) calculation reveals significant contribution of the metal cluster center to the unoccupied molecular orbitals in **3**, which is consistent with the experimental result of strong interfullerene electronic communication via the Rh_6 metal cluster spacer.

Introduction

Considerable research efforts have been devoted to the electrochemical studies of various [60]fullerene derivatives due to the ability of C_{60} to accept up to six electrons in a completely reversible manner.[1,2] In particular, bisfullerene compounds with two electroactive fullerene centers are of special interest, since the electronic communication between the two C_{60} moieties has practical implications for future optical and electronic applications.[3] A number of bisfullerene compounds with various spacers have been prepared and characterized in order to effect the electronic communication between the two C_{60} cages.[3] Weak through-space electronic communication, however, has been observed only for $C_{120}O$,[4] $C_{120}(CH_2)_2$,[5] $C_{120}C$,[6] and $C_{120}Si(C_6H_5)_2$,[7] where the fullerenes are directly bonded to each other or are separated by a single atom spacer. For organic-based bisfullerenes with longer spacers, no electronic communication has been observed. Insertion of organic spacers between the two C_{60} cages results in the transformation of the hybridization of C_{60} carbon atoms involved in the spacer binding from sp^2 to sp^3, and consequently the electronic communication can occur only through space via overlapped π-orbitals between the two separate C_{60} cages.

Metal cluster complexes of C_{60} exhibit remarkable thermal and electrochemical stabilities and strong electrochemical interaction between the two electroactive C_{60} and metal cluster

† Department of Chemistry, Korea University.
‡ National Research Laboratory, Department of Chemistry and School of Molecular Science (BK 21), Korea Advanced Institute of Science and Technology.

(1) (a) Dubois, D.; Kadish, K. M.; Flanagan, S.; Wilson, L. J. *J. Am. Chem. Soc.* **1991**, *113*, 7773−7774. (b) Xie, Q.; Perez-Cordero, E.; Echegoyen, L. *J. Am. Chem. Soc.* **1992**, *114*, 3978−3980. (c) Zhou, F.; Jehoulet, C.; Bard, A. J. *J. Am. Chem. Soc.* **1992**, *114*, 11 004−11 006.
(2) (a) Echegoyen, L.; Echegoyen, L. E. *Acc. Chem. Res.* **1998**, *31*, 593−601. (b) Martin, N.; Sanchez, L.; Illescas, B.; Perez, I. *Chem. Rev.* **1998**, *98*, 2527−2548.
(3) (a) Hummelen, J. C.; Knight, B.; Pavlovich, J.; González, R.; Wudl, F. *Science* **1995**, *269*, 1554−1556. (b) Wang, G.-W.; Komatsu, K.; Murata, Y.; Shiro, M. *Nature*, **1997**, *387*, 583−586. (c) Segura, J. L.; Martin, N. *Chem. Soc. Rev.* **2000**, *29*, 13−25. (d) Isobe, H.; Ohbayashi, A.; Sawamura, M.; Nakamura, E. *J. Am. Chem. Soc.* **2000**, *122*, 2669−2670. (e) Lebedkin, S.; Hull, W. E.; Soldatov, A.; Renker, B.; Kappes, M. M. *J. Phys. Chem. B* **2000**, *104*, 4101−4110. (f) Komatsu, K.; Fujiwara, K.; Murata, Y. *Chem. Commun.* **2000**, 1583−1584.
(4) Balch, A. L.; Costa, D. A.; Fawcett, R.; Winkler, K. *J. Phys. Chem.* **1996**, *100*, 4823−4827.
(5) Dragoe, N.; Shimotani, H.; Hayashi, M.; Saigo, K.; de Bettencourt-Dias, A.; Balch, A. L.; Miyake, Y.; Achiba, Y.; Kitazawa, K. *J. Org. Chem.* **2000**, *65*, 3269−3273.
(6) Dragoe, N.; Shimotani, H.; Wang J.; Iwaya, M.; de Bettencourt-Dias, A.; Balch, A. L.; Kitazawa, K. *J. Am. Chem. Soc.* **2001**, *123*, 1294−1301.
(7) Fujiwara, K.; Komatsu, K. *Org. Lett.* **2002**, *4*, 1039−1041.

centers. Furthermore, the electronic communication between C_{60} and metal cluster centers can be readily fine-tuned with ligands attached to the metal clusters.[8] The metal-C_{60} π-interaction in the C_{60}-metal moieties little perturbs the C_{60} hybridization as evidenced by earlier studies on self-assembled monolayers[9] and X-ray structural characterization of C_{60}-metal π-complexes,[10−12] which implies that the electronic properties of bisfullerene complexes with a metal cluster spacer are drastically different from those of organic-based bisfullerenes. In addition, C_{60}-metal cluster sandwich compounds should serve as direct models for two carbon nanotubes connected by a heterogeneous inorganic junction.[13] Multiple coordination of C_{60} to a single metal center, however, has not been accomplished prior to our study, even though C_{60} with a cone angle of 120° is not an exceptionally bulky ligand.[14] Coordination of two electron-withdrawing C_{60} ligands on a single metal center has been considered to be energetically unfavorable.

We have demonstrated that electron-withdrawing C_{60} cages can be connected by a cluster bridge (Rh_6 or Ir_4), when the cluster bridge is coordinated with electron-donating phosphine ligands.[15,16] The bisfullerene-metal cluster sandwich complexes, $Rh_6(CO)_5(dppm)_2(CNR)(\mu_3\text{-}\eta^2,\eta^2,\eta^2\text{-}C_{60})_2$[15] and $Ir_4(CO)_3(\mu_4\text{-}CH)(PMe_3)_2(\mu\text{-}PMe_2)(CNR)(\mu\text{-}\eta^2,\eta^2\text{-}C_{60})(\mu_4\text{-}\eta^1,\eta^1,\eta^2,\eta^2\text{-}C_{60})$[16] (R = $CH_2C_6H_5$), show the presence of unusually strong electronic communication between the two C_{60} centers, which is far stronger than that observed for organic-based bisfullerenes. To understand the nature of this strong inter-fullerene communication, we have carried out molecular orbital calculations on a set of face-capping $C_{60}-Rh_6$ cluster compounds, $Rh_6(CO)_9(dppm)_2(\mu_3\text{-}\eta^2,\eta^2,\eta^2\text{-}C_{60})$ (**1**), $Rh_6(CO)_7(dppm)_2(CNR)_2(\mu_3\text{-}\eta^2,\eta^2,\eta^2\text{-}C_{60})$ (**2**), and $Rh_6(CO)_5(dppm)_2(CNR)(\mu_3\text{-}\eta^2,\eta^2,\eta^2\text{-}C_{60})_2$ (**3**), in conjunction with their electrochemical property measurements by cyclic voltammetry. Herein, we report full details of synthesis, characterization, and electrochemical behaviors of **1**−**3** as well as their theoretical considerations.

Result and Discussion

Synthesis and Characterization of 1−3. When a mixture of $Rh_6(CO)_{12}(dppm)_2$[17] and 1.4 equiv. of C_{60} in chlorobenzene was heated at 120 °C, the color of the reaction mixture changed over 2 h from dark red to green. Removal of the solvent in vacuo and subsequent purification by column chromatography (silica gel, CS_2/CH_2Cl_2 = 4/1) gave a major green solid (**1**, 73%) following a purple band of unreacted C_{60}. Reaction of **1** with 10 equiv. of CNR (R = $CH_2C_6H_5$) in chlorobenzene at 80 °C slowly changed the solution from green to brown color over 1h. Removal of the solvent and purification by TLC (silica gel, CS_2/CH_2Cl_2 = 4/1) provided a greenish brown solid (**2**, R_f = 0.1, 59%) as the major product along with several uncharacterized minor bands at lower R_f values. The two new compounds were formulated as $Rh_6(CO)_9(dppm)_2(C_{60})$ (**1**) and $Rh_6(CO)_7(dppm)_2(CNR)_2(C_{60})$ (**2**) on the basis of microanalytical and positive FAB mass spectroscopic data.

Reaction of **1** with 4 equiv. of C_{60} in refluxing chlorobenzene for 3 h formed a new green compound identified by analytical TLC (silica gel), which could not be further characterized because of its marginal solubility after solvent removal. The reaction mixture was treated in situ with 1 equiv. of CNR at room temperature for 90 min. Removal of the solvent and purification by preparative TLC (silica gel, CS_2/CH_2Cl_2 = 7/1) provided a green solid **3** as the major product (R_f = 0.3, 31%). Compound **3** exhibited increased solubility and was formulated as $Rh_6(CO)_5(dppm)_2(CNR)(C_{60})_2$ on the basis of microanalytical data and X-ray crystallographic study (vide infra).

The ^{31}P NMR spectrum of **1** shows four multiplet signals of equal intensities at δ 18.68, 13.94, 10.99, and 8.56 for four phosphorus atoms of the two dppm ligands, indicating lack of symmetry in the molecule. The phosphorus resonances of **2** and **3** in the ^{31}P NMR spectra are extensively overlapped, which renders the peak assignment impossible. The ^1H NMR spectrum of **2**, however, shows four multiplets at δ 5.05, 4.89, 4.43, and 4.17 for the two sets of two diastereotopic methylene hydrogens in two dppm ligands and two AB patterns at δ 5.05 (J_{AB} = 16.7 Hz) and 4.70 (J_{AB} = 16.6 Hz) for the two sets of two diastereotopic benzylic hydrogens in two inequivalent benzyl isocyanide ligands. The ^1H NMR spectrum of **3** exhibits four multiplets at δ 5.33, 4.90, 4.57, and 3.96 for the four diastereotopic methylene hydrogens in two dppm ligands and an AB pattern at δ 5.06 (J_{AB} = 16.7 Hz) for the two diastereotopic benzylic hydrogens in the benzyl isocyanide ligand.

X-ray Crystallographic Studies of 1−3. Selected crystallographic details for **1**, **2**, and **3** are shown in Table 1. The metal−metal bond lengths and the selected distances for the C_{60} ligands are listed in Tables 2 and 3, respectively.

Compound **1** has two symmetrically unrelated, but nearly identical, molecular units in the crystal lattice, and one of them is shown in Figure 1. The Rh_6 octahedral metal framework of the starting material $Rh_6(CO)_{12}(dppm)_2$ remains intact, and the C_{60} ligand is face-capping Rh1−Rh2−Rh3 triangle as a $\mu_3\text{-}\eta^2,\eta^2,\eta^2$-ligand. The geometries for the remaining ligands are similar to those in $Rh_6(CO)_{12}(dppm)_2$.[17]

One dppm ligand bridges the Rh3−Rh4 edge and the other dppm ligand the Rh5−Rh6 edge. Four face-capping μ_3-CO ligands are observed and remaining carbonyls are all terminally

(8) (a) Song, H.; Lee, K.; Park, J. T.; Choi, M.-G. *Organometallics* **1998**, *17*, 4477−4483. (b) Song, H.; Lee, Y.; Choi, Z.-H.; Lee, K.; Park, J. T.; Kwak, J.; Choi, M.-G. *Organometallics* **2001**, *20*, 3139−3144. (c) Babcock, A. J.; Li, J.; Lee, K.; Shapley, J. R. *Organometallics* **2002**, *21*, 3940−3946.
(9) Cho, Y.-J.; Song, H.; Lee, K.; Kim, K.; Kwak, J.; Kim, S.; Park, J. T. *Chem. Commun.* **2002**, 2966−2967.
(10) (a) Fagan, P. J.; Calabrese, J. C.; Malone, B. *Science* **1991**, *252*, 1160−1161. (b) Balch, A. L.; Catalano, V. J.; Lee, J. W. *Inorg. Chem.* **1991**, *30*, 3980−3981. (c) Fagan, P. J.; Calabrese, J. C.; Malone, B. *J. Am. Chem. Soc.* **1991**, *113*, 9408−9409. (d) Bashilov, V. V.; Petrovskii, P. V.; Sokolov, V. I.; Lindeman, S. V.; Guzey, I. A.; Struchkov, Y. T. *Organometallics* **1993**, *12*, 991−992. (e) Balch, A. L.; Lee, J. W.; Noll, N. C.; Olmstead, M. M. *Inorg. Chem.* **1993**, *32*, 3577−3578. (f) Hsu, H.-F.; Du, Y.; Albrecht-Schmitt, T. E.; Wilson, S. R.; Shapley, J. R. *Organometallics* **1998**, *17*, 1756−1761.
(11) (a) Rasinkangas, M.; Pakkanen, T. T.; Pakkanen, T. A.; Ahlgrén, M.; Rouvinen, J. *J. Am. Chem. Soc.* **1993**, *115*, 4901. (b) Mavunkal, I. J.; Chi, Y.; Peng, S.-M.; Lee, G.-H. *Organometallics* **1995**, *14*, 4454−4456.
(12) (a) Hsu, H.-F.; Shapley, J. R. *J. Am. Chem. Soc.* **1996**, *118*, 9192−9193. (b) Lee, K.; Hsu, H.-F.; Shapley, J. R. *Organometallics* **1997**, *16*, 3876−3877. (c) Lee, K.; Shapley, J. R. *Organometallics* **1998**, *17*, 3020−3026. (d) Lee, K.; Lee, C. H.; Song, H.; Park, J. T.; Chang, H. Y.; Choi, M.-G. *Angew. Chem., Int. Ed.* **2000**, *39*, 1801−1804. (e) Lee, K.; Choi, Z.-H.; Cho Y.-J.; Song, H.; Park, J. T. *Organometallics* **2001**, *20*, 5564−5570. (f) Lee, K.; Song, H.; Park, J. T. *Acc. Chem. Res.* **2003**, *36*, 78−86.
(13) (a) Zhang, Y.; Ichihashi, T.; Landree, E.; Nihey, F.; Iijima, S. *Science* **1999**, *285*, 1719−1722. (b) Hermans, S.; Sloan, J.; Shephard, D. S.; Johnson, B. F. G.; Green, M. L. H. *Chem. Commun.* **2002**, 276−277.
(14) Balch, A. L. In *Applications of Organometallic Chemistry in the Preparation and Processing of Advanced Materials*; Harrod, J. F., Laine, R. M., Eds.; Kluwer Academic Publishers: Boston, MA, 1995; p283.
(15) Lee, K.; Song, H.; Kim, B.; Park, J. T.; Park, S.; Choi, M.-G. *J. Am. Chem. Soc.* **2002**, *124*, 2872−2873.
(16) Lee, G.; Cho, Y.-J.; Park, B. K.; Lee, K.; Park, J. T. *J. Am. Chem. Soc.* **2003**, *125*, 13 920−13 921.
(17) Foster, D. F.; Nicholls, B. S.; Smith, A. K. *J. Organomet. Chem.* **1982**, *236*, 395−402.

Table 1. Crystallographic Data for **1**, **2**, and **3**

t	1	2	3
formula	$C_{119}H_{44}O_9P_4Rh_6$	$C_{133}H_{58}N_2O_7P_4Rh_6$	$C_{183}H_{47}NO_5P_4Rh_6 \cdot C_6H_4Cl_2 \cdot 2H_2O$
fw	2358.88	2537.15	3415.84
cryst system	triclinic	triclinic	monoclinic
space group	$P\bar{1}$	$P\bar{1}$	$P2(1)/n$
a, Å	15.499(3)	14.678(1)	17.59(3)
b, Å	19.415(4)	20.035(1)	23.98(5)
c, Å	33.223(7)	20.336(1)	31.90(6)
α, deg.	85.07(3)	95.625(1)	90
β, deg.	83.43(3)	96.939(1)	96.75(4)
γ, deg.	73.24(3)	111.310(1)	90
V, Å^3	9495(3)	5465(1)	13360(45)
Z	4	2	4
D_{calcd}, g cm^{-3}	1.650	1.542	1.698
T, K	293(2)	293(2)	293(2)
λ (Mo Kα), Å	0.71073	0.71073	0.71073
μ, mm^{-1}	1.149	1.003	0.944
no. of rflns measd	32181	20146	109452
no. of unique rflns	19943	12924	18592
R_{int}	0.1894	0.0860	0.3367
goodness of fit	0.941	1.040	1.091
R_1[a]	0.1036	0.1029	0.0848
w$R2$[b]	0.2154	0.2873	0.2290

[a] $R_1 = \sum||F_o| - |F_c||/\sum|F_o|$. [b] $R_w = [\sum\omega(F_o^2 - F_c^2)^2/\sum\omega(F_o^2)^2]^{1/2}$.

Table 2. Metal-Metal Distances (Å) for **1**, **2**, and **3** (**1′** Denotes the Symmetrically Unrelated Molecule in the Crystal Lattice of **1**)

	1	1′	2	3
Rh1−Rh2	2.734(4)	2.751(4)	2.774(2)	2.690(4)
Rh1−Rh3	2.725(4)	2.730(4)	2.769(2)	2.649(5)
Rh1−Rh4	2.770(4)	2.795(4)	2.808(2)	2.676(5)
Rh1−Rh5	2.792(4)	2.786(4)	2.813(2)	2.698(5)
Rh2−Rh3	2.768(4)	2.772(4)	2.802(2)	2.743(4)
Rh2−Rh5	2.785(4)	2.771(4)	2.830(2)	2.760(4)
Rh2−Rh6	2.790(4)	2.794(4)	2.861(2)	2.772(5)
Rh3−Rh4	2.732(4)	2.722(4)	2.748(2)	2.746(4)
Rh3−Rh6	2.860(4)	2.868(4)	2.881(2)	2.793(6)
Rh4−Rh5	2.757(4)	2.759(4)	2.810(2)	2.757(4)
Rh4−Rh6	2.789(4)	2.799(4)	2.837(2)	2.751(4)
Rh5−Rh6	2.765(4)	2.768(4)	2.813(2)	2.764(5)

bonded. One μ_3-CO ligand is capping the Rh(4, 5, 6) triangle which is trans to the C_{60} coordinated on the Rh(1, 2, 3) triangle, and the other three μ_3-CO ligands are disposed in a fashion to form a tetrahedron composed of four μ_3-CO ligands as observed in $Rh_6(CO)_{12}(dppm)_2$.[17] The molecular structure of **2** is shown in Figure 2, and the general structural feature is similar to that of compound **1**. The only difference is that two terminal carbonyl ligands on Rh2 and Rh4 are displaced by two terminal CNR ligands. The Rh−C (C_{60}) distances in **2** do not alternate in length, while the C−C distances of the ligated C_6 ring of C_{60} ligand reveal bond alternation (av. 1.45 and 1.50 Å, respectively). Overall, the bonding parameters for the μ_3-η^2,η^2,η^2-C_{60} ligands in **1** and **2** are similar to those in other related μ_3-η^2,η^2,η^2-C_{60} cluster systems.[12]

The molecular structure of **3** is shown in Figure 3. The two μ_3-η^2,η^2,η^2-C_{60} ligands are face-capping Rh(1, 2, 3) and Rh(1, 4, 5) triangles, respectively, of the Rh_6 octahedral metal framework. The coordination environments of the two C_{60} ligands are different from each other; the Rh(1, 2, 3) triangle is coordinated by an isocyanide ligand and a phosphorus atom (P(1)) of a dppm ligand, while the Rh(1, 4, 5) triangle is coordinated by two phosphorus atoms (P(2,3)), each from the two dppm ligands. Interestingly, the Rh1 atom is bonded to both of the face-capping C_{60} ligands in an η^2- mode. Although the Rh1 atom is coordinated by two C_{60} ligands, the Rh1−C (C_{60}) bond distances (Rh1−C1 = 2.18(2) Å; Rh1−C2 = 2.18(1) Å; Rh1−C1′ = 2.15(2) Å; Rh1−C2′ = 2.14(2) Å) are comparable to the other Rh−C (C_{60}) distances (av. 2.18 Å) in **3**, implying that the electron-deficient nature of C_{60} is much compensated for by the remote CNR and dppm donor ligands. The ligated C_6 ring of the C_{60} ligand on Rh(1, 2, 3) triangle shows alternation in C−C bond distances (av. 1.45 and 1.48 Å, respectively), but no systematic bond alternation is observed either in the C_6 ring of the other C_{60} ligand on the Rh(1, 4, 5) triangle or in the Rh−C (C_{60}) distances. A terminal isocyanide ligand is coordinated on the Rh2 atom, and the geometries for the remaining ligands are similar to those in **1** and **2**.

Table 3. Selected Interatomic Distances (Å) for C_{60} Ligand in **1**, **2**, and **3** (**1′** Denotes the Symmetrically Unrelated Molecule in the Crystal Lattice of 1)

	1	1′	2
Rh1−C1	2.19(3)	2.24(3)	2.23(2)
Rh1−C2	2.19(3)	2.13(3)	2.18(2)
Rh2−C3	2.20(3)	2.17(3)	2.14(2)
Rh2−C4	2.13(3)	2.16(3)	2.20(2)
Rh3−C5	2.17(3)	2.10(3)	2.24(2)
Rh3−C6	2.18(3)	2.19(3)	2.22(2)
C1−C2	1.35(4)	1.46(4)	1.48(2)
C2−C3	1.53(4)	1.53(4)	1.51(2)
C3−C4	1.42(4)	1.41(4)	1.44(2)
C4−C5	1.49(4)	1.58(4)	1.48(2)
C5−C6	1.47(4)	1.45(4)	1.42(2)
C6−C1	1.43(4)	1.61(4)	1.53(2)
	3		
Rh1−C1	2.19(2)	Rh1−C1′	2.14(2)
Rh1−C2	2.20(1)	Rh1−C2′	2.15(2)
Rh2−C3	2.17(1)	Rh4−C3′	2.21(2)
Rh2−C4	2.14(2)	Rh4−C4′	2.19(2)
Rh3−C5	2.19(2)	Rh5−C5′	2.21(2)
Rh3−C6	2.19(1)	Rh5−C6′	2.19(2)
C1−C2	1.42(2)	C1′−C2′	1.45(2)
C2−C3	1.49(2)	C2′−C3′	1.42(2)
C3−C4	1.41(2)	C3′−C4′	1.40(2)
C4−C5	1.49(2)	C4−C5′	1.48(2)
C5−C6	1.36(2)	C5′−C6′	1.42(2)
C6−C1	1.48(2)	C6′−C1′	1.50(2)

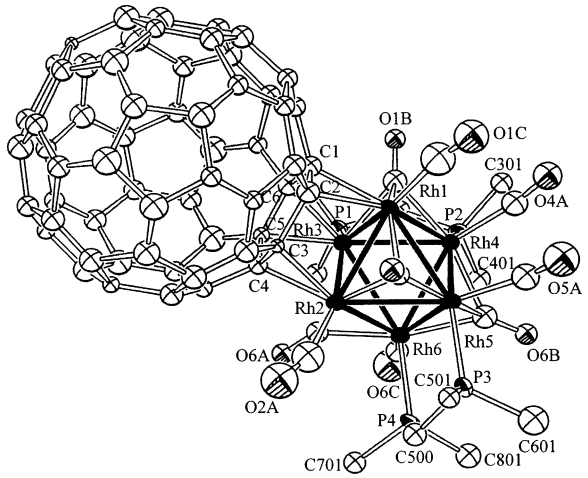

Figure 1. Molecular geometry and atomic-labeling scheme for **1**. Phenyl groups except ipso carbons are removed for clarity.

Electrochemical Studies. Electrochemical properties of $Rh_6(CO)_{12}(dppm)_2$, **1**, **2**, **3** as well as $Os_3(CO)_8(PPh_3)(\mu_3$-η^2,η^2,η^2-$C_{60})$ [8a] and $Os_3(CO)_8(CNCH_2C_6H_5)(\mu_3$-$\eta^2,\eta^2,\eta^2$-$C_{60})$[18] in chlorobenzene have been examined by cyclic voltammetry with

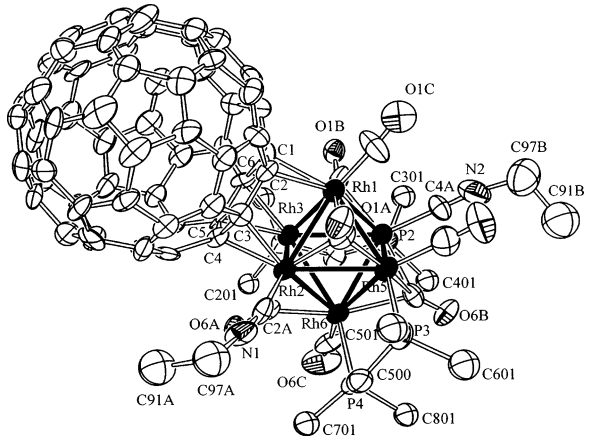

Figure 2. Molecular geometry and atomic-labeling scheme for **2**. Phenyl groups except ipso carbons are removed for clarity.

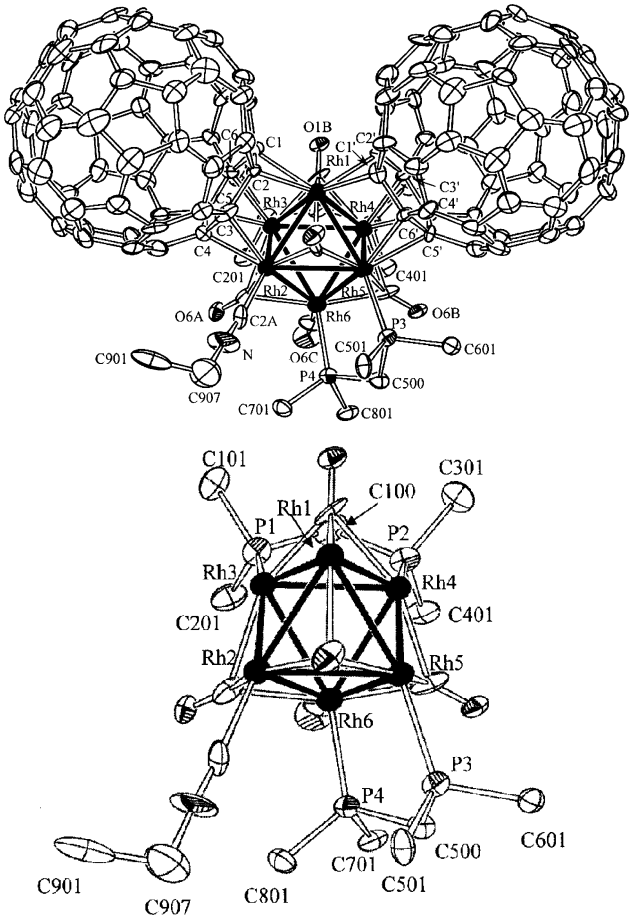

Figure 3. Top: Molecular geometry and atomic-labeling scheme for **3**. Phenyl groups except ipso carbons are removed for clarity. Bottom: Expanded view of the cluster core.

tetrabutylammonium perchlorate as the supporting electrolyte. Cyclic voltammograms (CVs) of $Rh_6(CO)_{12}(dppm)_2$, **1**, and **2** are shown in Figure 4 and that of **3** is shown Figure 5. Half-wave potentials ($E_{1/2}$) of free C_{60}, $Rh_6(CO)_{12}(dppm)_2$, **1**, **2**, and **3** are summarized in Table 4.

The CVs of both **1** and **2** exhibits similar four reversible redox couples up to $\mathbf{1}^{5-}$ and $\mathbf{2}^{5-}$ within the solvent potential window. The first two and the fourth redox waves are due to one-electron

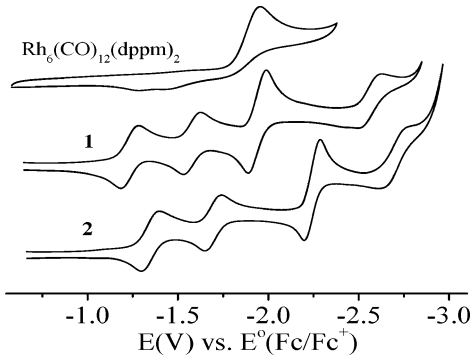

Figure 4. CVs of $Rh_6(CO)_{12}(dppm)_2$, **1**, and **2** in chlorobenzene (scan rate = 10 mV/s).

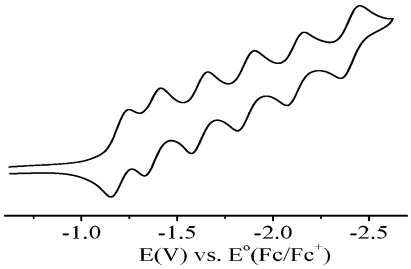

Figure 5. CV of compound **3** in chlorobenzene (scan rate = 10 mV/s).

Table 4. Half-Wave Potentials ($E_{1/2}$ vs $E^{\circ}_{Fc/Fc+}$) of C_{60}, $Rh_6(CO)_{12}(dppm)_2$, **1**, **2**, and **3** in Chlorobenzene

compound	$E_{1/2}{}^1$	$E_{1/2}{}^2$	$E_{1/2}{}^3$	$E_{1/2}{}^4$	$E_{1/2}{}^5$	$E_{1/2}{}^6$
C_{60}	−1.06	−1.43	−1.91	−2.38		
$Rh_6(CO)_{12}(dppm)_2$	−1.96[a,b]					
1	−1.23	−1.58	−1.94[a]	−2.57		
2	−1.35	−1.70	−2.25 [a]	−2.71		
3	−1.19	−1.38	−1.62	−1.86	−2.12	−2.41

[a] Two-electron process. [b] Peak potential of irreversible process.

processes, but the third redox wave corresponds to a two-electron process. The first two reductions for **1** and **2** occur at much more positive potentials compared to those of the Rh_6 metal center ($E_{red} = -1.96$ V for the parent molecule $Rh_6(CO)_{12}(dppm)_2$), and thus can be confidently assigned to the C_{60}-localized successive reductions. The first two waves of **1** are shifted to more negative potentials by 0.17 and 0.15 V, respectively, relative to those of free C_{60}. Such cathodic shifts are consistent with the presence of strongly electron-donating dppm ligands. The first two waves of **2** are further shifted to more negative potentials by 0.12 V compared to **1**, respectively, due to the additional donor effect of the two isocyanide ligands. The third (two-electron reduction) and the fourth (one-electron reduction) waves in **1** and **2** are assigned to the redox processes also localized at the C_{60} ligand, based on the molecular orbital calculation results of these molecules (vide infra). It is notable that complexes **1** and **2** demonstrate high electrochemical stability without showing a metal cluster reduction process within the solvent cutoff window. The CV of the parent molecule $Rh_6(CO)_{12}(dppm)_2$, however, exhibits a one-step two-electron reduction at −1.96 V and two consecutive oxidation steps (−1.42 and −1.29 V) at the Rh_6 metal center. Similar irreversible behaviors have been observed for several metal carbonyl clusters, where loss of a carbonyl and structural change are generally accompanied by the two-electron reduction step.[19] The face-capping μ_3-η^2,η^2,η^2-C_{60} bonding interaction, apparently, greatly alters the electronic nature of the Rh_6 cluster unit,

(18) Song, H.; Lee, C. H.; Lee, K.; Park, J. T. *Organometallics* **2002**, *21*, 2514−2520.

Table 5. Half-Wave potentials ($E_{1/2}$ vs $E^{\circ}_{Fc/Fc+}$) of C_{60}, $Os_3(CO)_9(\mu_3\text{-}\eta^2,\eta^2,\eta^2\text{-}C_{60})$ (**4**), $Os_3(CO)_8(PMe_3)(\mu_3\text{-}\eta^2,\eta^2,\eta^2\text{-}C_{60})$ (**5**), $Os_3(CO)_8(PPh_3)(\mu_3\text{-}\eta^2,\eta^2,\eta^2\text{-}C_{60})$ (**6**), and $Os_3(CO)_8(CNR)(\mu_3\text{-}\eta^2,\eta^2,\eta^2\text{-}C_{60})$ (**7**) in Chlorobenzene

compound	$E_{1/2}{}^1$	$E_{1/2}{}^2$	ref
C_{60}	−1.06	−1.43	this work
4	−0.98	−1.33	8a
5	−1.06	−1.42	8a
6	−1.07	−1.43	this work
7	−1.06	−1.43	this work

resulting in the observed C_{60}-localized reductions and high electrochemical stabilities of **1** and **2**. Similar increased electrochemical stability has been previously demonstrated for related C_{60}-metal cluster complexes with a face-capping μ_3-η^2,η^2,η^2-C_{60} ligand.[8a,b]

The CV of **3** exhibits six well-separated reversible, one-electron redox waves as shown in Figure 5. Each redox wave of **3** is ascribed to sequential, pairwise addition of six electrons into the two C_{60} centers to form $C_{60}{}^{-}-Rh_6-C_{60}$, $C_{60}{}^{-}-Rh_6-C_{60}{}^{-}$, $C_{60}{}^{2-}-Rh_6-C_{60}{}^{-}$, ..., and ultimately $C_{60}{}^{3-}-Rh_6-C_{60}{}^{3-}$. All three pairs of redox waves are shifted to more negative potentials (0.13 and 0.32 V; 0.19 and 0.43 V; 0.21 and 0.50 V) relative to free C_{60}. The absence of Rh_6 cluster reduction wave for **3** in the solvent window could be explained by significant decrease in electron affinity of the cluster framework due to coordination of two, electron-rich polyanionic C_{60} ligands, which are generated during electrochemical studies. This observation suggests a strong electronic communication between the metal cluster and C_{60} centers. There is little difference between donor effects of a phosphine ligand and a benzyl isocyanide ligand in C_{60}-metal cluster complexes, which lead to the negative shifts (0.08∼0.09 V) of C_{60} reduction potentials compared to the parent carbonyl complex; $Os_3(CO)_9(\mu_3\text{-}\eta^2,\eta^2,\eta^2\text{-}C_{60})$, $Os_3(CO)_8(PMe_3)(\mu_3\text{-}\eta^2,\eta^2,\eta^2\text{-}C_{60})$, $Os_3(CO)_8(PPh_3)(\mu_3\text{-}\eta^2,\eta^2,\eta^2\text{-}C_{60})$, and $Os_3(CO)_8(CNCH_2C_6H_5)(\mu_3\text{-}\eta^2,\eta^2,\eta^2\text{-}C_{60})$ exhibit C_{60}-localized first redox wave ($E_{1/2}{}^{0/-1}$) at −0.98, −1.06, −1.07, and −1.06 V, respectively, as shown in Table 5. The donor effect of a phosphorus end of a dppm ligand should be very similar to that of a benzyl isocyanide ligand, and thus the electronic environment for the two C_{60} centers is essentially the same despite the difference in coordination spheres around the two C_{60} centers. The large peak separations ($\Delta(E_{1/2}{}^1, E_{1/2}{}^2) = 0.19$ V, $\Delta(E_{1/2}{}^3, E_{1/2}{}^4) = 0.24$ V, $\Delta(E_{1/2}{}^5, E_{1/2}{}^6) = 0.29$ V) in the three redox pairs of the two C_{60} ligands, therefore, reflect a strong electronic communication between the two C_{60} centers via the Rh_6 spacer. Much smaller peak separations ($\Delta(E_{1/2}{}^1, E_{1/2}{}^2) = 0.09$ V, $\Delta(E_{1/2}{}^3, E_{1/2}{}^4) = 0.08$ V, $\Delta(E_{1/2}{}^5, E_{1/2}{}^6) = 0.14$ V) have been observed for $C_{120}Si(C_6H_5)_2$[7], which represents the strongest electronic interaction reported for noncluster-bridged bisfullerene compounds.

Theoretical Calculations of 1−3. Density functional theory (DFT) using B3LYP[20] hybrid functional was employed to investigate the molecular orbitals of fullerene-metal complex compounds, **1**, **2**, and **3**, in an effort to understand electrochemical properties of these complexes.

Table 6. DFT Calculation Results for **1** and **2**

orbital no.	orbital energy (eV)	C_{60} character (%)	cluster character (%)
	1		
499(LUMO + 2)	−2.5062	91	9
498(LUMO + 1)	−2.7995	85	15
497(LUMO)	−2.9767	89	11
496(HOMO)	−4.9285	19	81
	2		
547(LUMO + 2)	−2.3862	89	11
546(LUMO + 1)	−2.5157	92	8
545(LUMO)	−2.8305	83	17
544(HOMO)	−4.4834	17	83

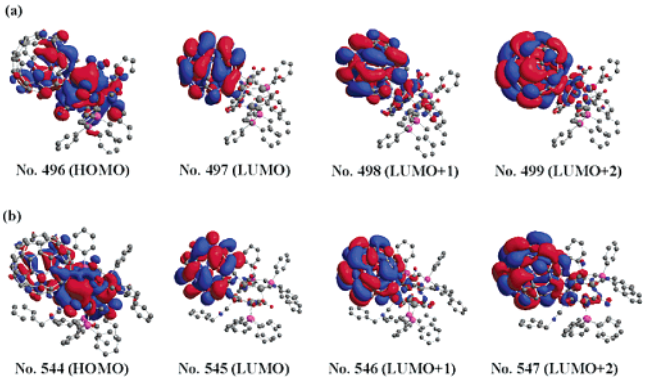

Figure 6. Diagrams for frontier MOs of **1**(a) and **2**(b).

Table 6 shows energies and contribution of component parts for selected molecular orbitals (MOs) of monofullerene complexes, **1** and **2**. The diagrams for MOs of **1** and **2** are displayed in Figure 6 and the similarity between both sets of MOs is clearly seen. Highest occupied molecular orbitals (HOMOs) for both compounds are mainly metal cluster-based, but with nonnegligible atomic orbital contributions (19% (**1**) and 17% (**2**)) from metal bonded carbon atoms in the C_{60} unit, which implies a strong ground-state interaction between C_{60} and Rh_6 cluster centers. The unoccupied MOs are C_{60}-based, but the metal cluster contributions to these MOs are not negligible (11%, 15%, and 9% for **1**; 17%, 8%, and 11% for **2**; see Table 6). Metal cluster contribution to C_{60}-based unoccupied orbitals to a similar extent has been previously reported for a related C_{60}-cluster complex $Ru_3(CO)_9(\mu_3\text{-}\eta^2,\eta^2,\eta^2\text{-}C_{60})$.[21]

The four reversible redox waves of **2** (Figure 4) are shifted to negative potentials by 0.12, 0.12, 0.31, and 0.14 V as compared to those of **1** due to the presence of electron-donating benzylisocyanide ligands. While the values of negative potential shift for the three one-electron redox waves are similar to one another, the shift value of 0.31 V for the third, one-step two-electron reduction wave in **2** is abnormally high. Assuming that the C_{60}-based unoccupied orbitals are sequentially filled by added electrons, this behavior could be rationalized by comparing the energies of unoccupied orbitals of the two compounds as following. The LUMO and LUMO + 1 are responsible for the first two one-electron and the third two-electron reduction steps, respectively. Much larger energy difference was observed between LUMO (orbital No. 545) and LUMO + 1 (orbital No. 546) of **2** compared to those (orbitals No. 497 and 498) of **1**:

(19) (a) Geiger, W. E.; Connelly, N. G. *Adv. Organomet. Chem.* **1985**, *24*, 87−130. (b) Johnson, B. F. G.; Lewis, J.; Nelson, W. J. H.; Nicholls, J. N.; Puga, J.; Raithby, P. R.; Rosales, M. J.; Schroder, M.; Vargas, M. D. *J. Chem. Soc., Dalton Trans.* **1983**, 2447−2457. (c) Clark, R. J. H.; Dyson, P. J.; Humphrey, D. G.; Johnson, B. F. G. *Polyhedron* **1998**, *17*, 2985−2991. (d) Shephard, D. S.; Johnson, B. F. G.; Harrison, A.; Parsons, S.; Smidt, S. P.; Yellowlees, L. J.; Reed, D. *J. Organomet. Chem.* **1998**, *563*, 113−136.
(20) Becke, A. D. *J. Chem. Phys.* **1993**, *98*, 5648−5652.
(21) Lynn, M. A.; Lichtenberger, D. L. *J. Cluster Sci.* **2000**, *11*, 169−188.

Table 7. DFT Calculation Results for **3**

orbital no.	orbital energy (eV)	C_{60} character (%)		cluster character (%)
		C_{60} (left)	C_{60} (right)	
685(LUMO + 5)	−2.1848	75	9	16
684(LUMO + 4)	−2.2509	4	80	16
683(LUMO + 3)	−2.3037	32	51	17
682(LUMO + 2)	−2.3511	61	28	11
681(LUMO + 1)	−2.4232	1	69	30
680(LUMO)	−2.5693	61	1	38
679(HOMO)	−4.3745	12	12	76

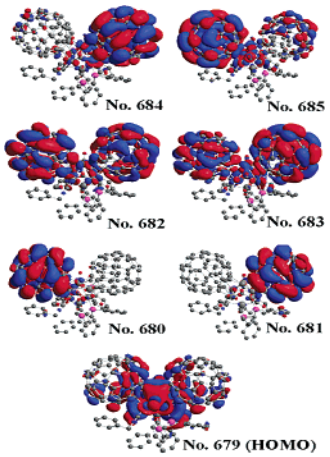

Figure 7. Diagrams for frontier MOs of **3**.

ΔE (orbitals No. 497, 498) = 0.1771 eV for **1** and ΔE (orbitals No. 545, 546) = 0.3148 eV for **2**.

Calculated results for selected MOs for **3** are shown in Table 7, and the diagrams for these MOs are depicted in Figure 7. The HOMO for **3** is mainly metal cluster-based (76%) with some atomic orbital contributions (12% and 12%) from metal bonded carbon atoms in the two C_{60} units as similarly observed for **1** and **2**. The unoccupied MOs are C_{60}-based, but again significant metal cluster contributions to the MOs are observed (38%, 30%, 11%, 17%, 16%, and 16%). In addition, contributions from the two C_{60} units show a pairwise behavior in the three sets of adjacent unoccupied MOs (No. 680 and 681; No. 682 and 683; No. 684 and 685), which explains the alternating electron additions to the two C_{60} units in **3**. The spin pairing energies, apparently, exceeds the energy gaps among unoccupied MOs of **3**.

The second redox wave in each pair in the CV of **3** (Figure 5) becomes increasingly separated from the first wave as the reduction proceeds ($\Delta(E_{1/2}^3, E_{1/2}^4) - \Delta(E_{1/2}^1, E_{1/2}^2) = 0.05$ V; $\Delta(E_{1/2}^5, E_{1/2}^6) - \Delta(E_{1/2}^3, E_{1/2}^4) = 0.05$ V). Similar trend was also observed in $C_{120}O$ [4] and $C_{120}(SiPh_2)$ [7] ($C_{120}O$: $\Delta(E_{1/2}^3, E_{1/2}^4) - \Delta(E_{1/2}^1, E_{1/2}^2) = 0.02$ V; $\Delta(E_{1/2}^5, E_{1/2}^6) - \Delta(E_{1/2}^3, E_{1/2}^4) = 0.08$ V; $C_{120}(SiPh_2)$: $\Delta(E_{1/2}^3, E_{1/2}^4) - \Delta(E_{1/2}^1, E_{1/2}^2) = -0.01$ V; $\Delta(E_{1/2}^5, E_{1/2}^6) - \Delta(E_{1/2}^3, E_{1/2}^4) = 0.06$ V), and was proposed to result from the effects of increasing Coulombic repulsion. The increase in the separation within the redox pairs of **3**, however, cannot be explained solely by the stronger Coulombic repulsion, because the increase in redox pair separation of $C_{120}O$[4] and $C_{120}(SiPh_2)$[7] with much shorter interfullerene distances of ~1.5 Å are only comparable, if not smaller. Careful examination of the MOs of **3** gives further insight on the observed electrochemical behavior of this compound. The significant metal cluster contributions of 38% and 30% to the MOs of No. 680 and No. 681, respectively, suggest that the electronic information of one C_{60} ligand is efficiently communicated through the Rh_6 cluster to the other C_{60} ligand. More interestingly, the two C_{60} ligands contribute more or less evenly to the higher lying MOs, No. 682 (61% and 28%) and No. 683 (32% and 51%), in conjunction with nonnegligible metal cluster contributions of 11% and 17%. The electrons in these MOs are delocalized over the entire molecule to result in stronger repulsion between electrons in these MOs, which in turn would lead to the observed large peak separation in the third redox pair in the CV of **3**. This delocalization was not anticipated in our earlier interpretation based on CV data alone.

Conclusion

Compounds **1** and **2** have been proposed to undergo C_{60}-localized reversible redox processes up to $\mathbf{1}^{5-}$ and $\mathbf{2}^{5-}$ within the solvent cutoff window, based on cyclic voltammetric studies and MO calculations. The bisfullerene metal sandwich complex **3** reveals an interesting structural feature of a Rh metal atom interconnecting two C_{60} cages and unusually strong electronic communication between the two C_{60} centers. The MO calculation of **3** reveals that the strong interfullerene electronic interaction has been possible by the strong contribution of the cluster unit, which acts as a passage for electronic communication, to the unoccupied MOs of this compound. The unique electronic behavior of the C_{60}-metal cluster sandwich compound and its theoretical consideration by MO calculation described herein should have a direct relevance to two carbon nanotubes connected by a heterogeneous inorganic junction, which might find useful applications in future electronic materials.

Experimental Section

General Comments. All reactions were carried out under a nitrogen atmosphere with use of standard Schlenk techniques.[22] Solvents were dried appropriately before use. C_{60} (99.5%, Southern Chemical Group, LLC.), $Rh_6(CO)_{16}$ (Strem Chemicals), and CNR (R = $CH_2C_6H_5$, Aldrich) were used without further purification. $Rh_6(CO)_{12}(dppm)_2$,[17] $Os_3(CO)_8(PPh_3)(\mu_3\text{-}\eta^2,\eta^2,\eta^2\text{-}C_{60})$,[8a] and $Os_3(CO)_8(CNR)(\mu_3\text{-}\eta^2,\eta^2,\eta^2\text{-}C_{60})$[18] were prepared by the literature methods. Preparative thin layer plates were prepared with silica gel GF_{254} (Type 60, E. Merck).

Infrared spectra were obtained on a Bruker EQUINOX-55 FT-IR spectrophotometer. ^{1}H (400 MHz) spectra were recorded on a Bruker Avance-400 spectrometer. ^{31}P (122 MHz) NMR spectra were recorded on a Bruker AM-300 spectrometer. All *m*/*z* values are referenced to ^{103}Rh.

Preparation of $Rh_6(CO)_9(dppm)_2(\mu_3\text{-}\eta^2,\eta^2,\eta^2\text{-}C_{60})$ (1). A chlorobenzene (150 mL) solution of $Rh_6(CO)_{12}(dppm)_2$ (600 mg, 0.339 mmol) and C_{60} (350 mg, 0.486 mmol) prepared in a 250 mL three-neck flask equipped with a reflux condenser was heated at 120 °C for 2 h. The solution color gradually changed from red to green. The solvent was removed under vacuum, and the dark residue dissolved in minimal amount of carbon disulfide was placed on top of a silica gel column (5 × 20 cm). Elution by CS_2/CH_2Cl_2 (4/1) afforded a brownish green solid of **1** (582 mg, 0.247 mmol, 73%) following a purple band of C_{60}. IR (CS_2) ν_{CO} 2029(vs), 2006(s), 1984(m), 1743(vs), 1719(vs) cm^{-1}; ^{1}H NMR (1,2-$C_6D_4Cl_2$, 298 K) δ 8.2−7.2 (m, 40H),

(22) Shriver, D. F.; Drezdzon, M. A. *The Manipulation of Air-Sensitive Compounds*, 2nd ed.; Wiley: New York, 1986.

5.03 (m, 1H), 4.75 (m, 1H), 4.32 (m, 1H), 4.21 (m, 1H); ^{31}P-{^{1}H} NMR (1,2-$C_6D_4Cl_2$, 298 K) δ 18.68 (m, 1P), 13.94 (m, 1P), 10.99 (m, 1P), 8.56(m, 1P); MS (FAB$^+$) *m*/*z* 2358 (M^+). Anal. Calcd. for $C_{119}H_{44}O_9P_4Rh_6$: C, 60.59; H, 1.88. Found: C, 60.34; H, 2.01.

Preparation of $Rh_6(CO)_7(dppm)_2(CNR)_2(\mu_3\text{-}\eta^2,\eta^2,\eta^2\text{-}C_{60})$ (R = $CH_2C_6H_5$) (2). A chlorobenzene (20 mL) solution of **1** (40.0 mg, 0.017 mmol) and CNR (20.0 mg, 0.171 mmol) was prepared in a 100 mL three-neck flask equipped with a reflux condenser. The reaction mixture was heated at 80 °C for 1 h, and the solution color slowly changed from green to brown. Solvent removal in vacuo and separation by TLC (silica gel, CS_2/CH_2Cl_2 (4/1)) gave a greenish brown solid of **2** (R_f = 0.1, 24.9 mg, 0.010 mmol, 59%) as the major product. IR (CH_2Cl_2) ν_{CO} 1996(s, sh), 1990(s), 1970(m, sh), 1734(vs), 1714(vs) cm^{-1} ν_{CN} 2160(m), 2138(w, sh) cm^{-1}; ^{1}H NMR (1,2-$C_6D_4Cl_2$, 298 K) δ 8.2−7.2 (m, 50H), 5.05 (2H, J_{AB} = 16.7 Hz, CNCH_2Ph), 5.05 (overlapped, m, 1H) 4.89 (m, 1H), 4.70 (2H, J_{AB} = 16.6 Hz, CNCH_2Ph), 4.43 (m, 1H), 4.17 (m, 1H); ^{31}P{^{1}H} NMR (1,2-$C_6D_4Cl_2$, 298 K) δ 19.37−8.37 (m, 4P); MS (FAB$^+$) *m*/*z* 2536 (M^+). Anal. Calcd. for $C_{133}H_{58}O_7N_2P_4Rh_6$: C, 62.96; H, 2.30; N, 1.10. Found: C, 62.64; H, 2.56; N, 0.98.

Preparation of $Rh_6(CO)_5(dppm)_2(CNR)(\mu_3\text{-}\eta^2,\eta^2,\eta^2\text{-}C_{60})_2$ (3). A chlorobenzene (50 mL) solution of **1** (50.0 mg, 0.021 mmol) and C_{60} (61.2 mg, 0.085 mmol 4equiv) prepared in a 100 mL three-neck flask equipped with a reflux condenser was heated at 132 °C for 3 h. The reaction mixture was cooled to room temperature. To the reaction mixture was added dropwise 1 equiv of CNR in 1 mL chlorobenzene, and the solution was stirred for 90 min. Solvent removal in vacuo and separation by TLC (silica gel, CS_2/CH_2Cl_2 (7/1)) gave a greenish brown solid of **3** (R_f = 0.3, 19.9 mg, 0.006 45 mmol, 31%) as the major product. IR (CS_2) ν_{CO} 1987 (s, br) cm^{-1}; ^{1}H NMR (1,2-$C_6D_4Cl_2$, 298 K) δ 8.4−6.9 (m, 45H), 5.33 (m, 1H), 5.06 (2H, J = 16.7 Hz, CNCH_2Ph), 4.90 (m, 1H), 4.57 (m, 1H), 3.96 (m, 1H); ^{31}P{^{1}H} NMR (1,2-$C_6D_4Cl_2$, 298 K) δ 18.3−12.9 (m, 3P), 5.96 (m, 1P); Anal. Calcd. for $C_{183}H_{51}O_5NP_4Rh_6$: C, 71.25; H, 1.67; N, 0.45. Found: C, 71.08; H, 2.01; N, 0.46.

X-ray Crystallographic Studies. Crystals of **1**, **2**, and **3** suitable for an X-ray analysis were grown by slow solvent diffusion; for **1** of heptane into carbon disulfide/chloroform (1/1) at room temperature, for **2** of methanol into carbon disulfide/1,2-dichlorobenzene (1/1) at room temperature, and for **3** of methanol into carbon disulfide/1,2-dichlorobenzene (1/1) at 10 °C. The data crystals were mounted on glass fibers, transferred to a Siemens SMART diffractometer/CCD area detector employing 3 kW sealed tube X-ray source operating at 2 kW, and centered in the beam. Data were collected at room temperature for 12 h. Preliminary orientation matrix and cell constants were determined with a set of 20 data frames with 30 s collection per frame, followed by spot integration and least-squares refinement. A hemisphere of data was collected using 0.3° ω scans at 30 s per frame. The raw data were integrated (XY spot spread = 1.60, Z spot spread = 0.6) and the unit cell parameters were refined using SAINT.[23] Data analysis and absorption correction were performed by using Siemens XPREP. The data were corrected for Lorentz and polarization effects, but no correction for crystal decay was applied. Details of the relevant crystallographic data are given in Table 1. The structures were determined by direct methods;[24] positions for the rhodium atoms were deduced from an E map. One cycle of isotropic least-squares refinement (SHLEX97) [25] followed by an unweighted difference Fourier synthesis revealed positions for the rhodium and remaining non-hydrogen atoms. Hydrogen atoms were not included in the final structure factor calculations. Successful convergence of full-matrix least-squares refinement on F^2 was indicated by the maximum shift/error for the final cycle. The final difference Fourier map had no significant features. The metal−metal distances and the selected distances for C_{60} ligands in **1**, **2**, and **3** are shown in Table 2 and Table 3, respectively.

Electrochemical Measurements. Cyclic voltammetry and chronoamperometry were carried out a BAS 100B (Bioanalytical Systems, Inc.) electrochemical analyzer using the conventional three electrode system of a platinum working electrode (1.6 mm diameter disk, Bioanalytical Systems, Inc.), a platinum counter wire electrode (5 cm length of 0.5 mm diameter wire), and a Ag/Ag^+ reference electrode (0.1 M $AgNO_3$/Ag in acetonitrile with a Vycor salt bridge). All measurements were performed at ambient temperature under nitrogen atmosphere in a dry deoxygenated 0.1 M chlorobenzene solution of $[(n\text{-}Bu)_4N]ClO_4$. The concentrations of compounds were ca. 3×10^{-4} M. All potentials were referenced to the standard ferrocene/ferrocenium (F_c/F_c^+) scale. Relative number of electrons involved in each reduction process was obtained from the graph of current vs (time)$^{-1/2}$ according to the Cottrell equation.[26]

Computational Details. Density functional theory (DFT) using B3LYP[20] hybrid functional was employed to investigate the molecular orbitals of fullerene-metal complex compounds. B3LYP functional has been widely used to calculate molecular orbitals of fullerene and fullerene-derivatives.[27,28] The coordinates for **1**, **2**, and **3** were taken directly from the respective crystal structures without further structural optimization.

To reduce the number of electrons treated, relativistic effective core potentials with corresponding basis sets were used for Rh atoms.[29] The 3-21+G* basis set was used for C, N, O, and P atoms. The carbon atoms of the C_{60} ligand were calculated using 6-311G* basis set for compounds **1** and **2** and 6-31G* basis set for **3**.

All DFT calculations were carried out with the GAUSSIAN98 program package.[30]

(23) *SAINT*, SAX Area-Detector Integration Program, Version 4.050; Siemens Analytical Instrumentation: Madison, WI, 1995.

(24) Sheldrick, G. M. *Acta Crystallogr*. **1990**, *A46*, 467−473.
(25) Sheldrick, G. M. *SHELX97*, Program for Crystal Structure Refinement; University of Göttingen: Germany, 1997.
(26) Bard, A. J.; Faulkner, L. R. *Electrochemical Methods*; John Wiley & Sons: New York, 1980; pp 142−146.
(27) Xie, R.-H.; Bryant, G. W.; Jensen, L.; Zhao, J.; Smith, V. H., Jr. *J. Chem. Phys*. **2003**, *118*, 8621−8635.
(28) Patchkovskii, S.; Thiel, W. *J. Am. Chem. Soc*. **1998**, *120*, 556−563.
(29) LaJohn, L. A.; Christiansen, P. A.; Ross, R. B.; Ermler, W. C. *J. Chem. Phys*. **1987**, *87*, 2812−2824.
(30) Frisch, M. J.; Trucks, G. W.; Schlegel, H. B.; Scuseria, G. E.; Robb, M. A.; Cheeseman, J. R.; Zakrzewski, V. G.; Montgomery, J. A., Jr.; Stratmann, R. E.; Burant, J. C.; Dapprich, S.; Millam, J. M.; Daniels, A. D.; Kudin, K. N.; Strain, M. C.; Farkas, O.; Tomasi, J.; Barone, V.; Cossi, M.; Cammi, R.; Mennucci, B.; Pomelli, C.; Adamo, C.; Clifford, S.; Ochterski, J.; Petersson, G. A.; Ayala, P. Y.; Cui, Q.; Morokuma, K.; Malick, D. K.; Rabuck, A. D.; Raghavachari, K.; Foresman, J. B.; Cioslowski, J.; Ortiz, J. V.; Stefanov, B. B.; Liu, G.; Liashenko, A.; Piskorz, P.; Komaromi, I.; Gomperts, R.; Martin, R. L.; Fox, D. J.; Keith, T.; Al-Laham, M. A.; Peng, C. Y.; Nanayakkara, A.; Gonzalez, C.; Challacombe, M.; Gill, P. M. W.; Johnson, B. G.; Chen, W.; Wong, M. W.; Andres, J. L.; Head-Gordon, M.; Replogle, E. S.; Pople, J. A. *Gaussian 98*, revision A.11; Gaussian, Inc.: Pittsburgh, PA, 1998.

Acknowledgment. K.L. thanks a Korea University Grant and Center for Electro- and Photo-Responsive Molecules for financial support of this research. Y.S.L. thanks the support by Center for Nanotubes and Nanostructured Composite and Center for Nanomechatronics and Manufacturing. J.T.P. thanks the National Research Laboratory (NRL) Program of Korean Ministry of Science & Technology (MOST) and the Korea Science Engineering Foundation (Project No. 1999-1-122-001-5).

Supporting Information Available: X-ray crystallographic files for **1**, **2**, and **3** (CIF). This material is available free of charge via the Internet at http://pubs.acs.org.

JA047290U